Journal of Alloys and Compounds 489 (2010) 394–400

Contents lists available at ScienceDirect

Journal of Alloys and Compounds

journal homepage: www.elsevier.com/locate/jallcom

Investigation of planetary milling for nano-silicon carbide reinforced aluminium metal matrix composites

Lauri Kollo[a,b,*], Marc Leparoux[a], Christopher R. Bradbury[a], Christian Jäggi[a], Efraín Carreño-Morelli[c], Mikel Rodríguez-Arbaizar[c]

[a] Laboratory of Advanced Materials Processing, EMPA, Feuerwerkerstrasse 39, 3602 Thun, Switzerland
[b] Department of Materials Engineering, Tallinn University of Technology, Ehitajate tee 5, 19086 Tallinn, Estonia
[c] University of Applied Sciences of Western Switzerland, Design & Materials Unit, 1950 Sion, Switzerland

ARTICLE INFO

Article history:
Received 11 August 2009
Received in revised form
22 September 2009
Accepted 23 September 2009
Available online 13 October 2009

Keywords:
Metal matrix composites
Powder metallurgy
Nanostructured materials
Mechanical alloying
Mechanical properties

ABSTRACT

High-energy planetary milling was used for mixing aluminium powders with 1 vol.% of silicon carbide (SiC) nanoparticles. A number of milling parameters were modified for constituting the relationship between the energy input from the balls and the hardness of the bulk nanocomposite materials. It was shown that mixing characteristics and reaction kinetics with stearic acid as process control agent can be estimated by normalised input energy from the milling bodies. For this, the additional parameter characterising the vial filling was determined experimentally. Depending on the ball size, a local minimum in filling parameter was found, laying at 25 or 42% filling of the vial volume for the balls with diameter of 10 and 20 mm, respectively. These regions should be avoided to achieve the highest milling efficiency. After a hot compaction, fourfold difference of hardness for different milling conditions was detected. Therewith the hardness of the Al–1 vol.% nanoSiC composite could be increased from 47 $HV_{0.5}$ of pure aluminium to 163 $HV_{0.5}$ when milling at the highest input energy levels.

1. Introduction

Aluminium-based metal matrix composites with small amount of nanometer-range (<0.1 μm) discontinuous hard phases as reinforcement have attracted considerable research interest during recent years due to the potential for the development of novel composites with unique mechanical and physical properties [1]. The primary challenge when producing nanocomposites by introducing pre-fabricated nanoparticles into the matrix is homogeneous dispersion of the reinforcement particles in the matrix. One perspective to achieve this is via a powder metallurgy route involving high-energy milling [2–6].

Mixing behavior of aluminium with hard nanophase powders by high-energy milling can be divided into three stages. Firstly, the powder is plastically deformed to form flake like structures. After a certain time of milling the powder is hardened up to a state that brittle fracture of the particles will occur and an equiaxial structure is formed. This is followed by a stable milling phase with the equilibrium between fracturing and welding of the particles [7–9].

The co-effect of varying process parameters of milling on the evolution of powder properties is not well understood yet. Several models have been proposed to describe the mechanisms of mixing ductile–ductile or ductile–brittle systems by high-energy milling. One of the approaches is by associating the global processing parameters to the properties of the processed powder product. This has enabled the construction of milling maps or energy maps for designing mechanical alloying or amorphisation of composite powders [10,11] or mechanical activation [12].

In this work, varying milling parameters, the effectiveness of mixing of silicon carbide nanoparticles with aluminium powder by planetary milling is investigated. The hardness of the compressed samples is taken as the qualitative factor of the efficiency to mix the composite powders. The energy transfer from the balls to the powder is estimated by input energy model. This is conducted by calculating the total input energy from multiple ball impacts. The final goal is to achieve the maximum hardness of the nanocomposites.

2. Theoretical background

Modelling of the planetary milling is needed in order to specify the role of different parameters on the energy transfer from the milling bodies to the powder. The milling process itself is a complex process, involving a number of variables that could only be approximately ascertained (e.g. the quantity of the powder entrapped

* Corresponding author at: Tallinn University of Technology, Department of Materials Engineering, Ehitajate tee 5, 19086 Tallinn, Estonia. Tel.: +372 620 3356; fax: +372 620 3196.
E-mail address: lauri.kollo@staff.ttu.ee (L. Kollo).

0925-8388/$ – see front matter © 2009 Elsevier B.V. All rights reserved.
doi:10.1016/j.jallcom.2009.09.128

between the milling bodies during the impact or friction coefficients between balls and vial surface during rolling). For this reason it is recommended to keep the milling models "simple", while still reflecting the fundamental physics of the process [13].

In this work, as the basis for estimating the energy input, the dynamics of single ball impacts in planetary mill were estimated. Secondly, the number of balls and the amount of powder were included to the model to obtain an estimation of the normalised input energy.

2.1. Dynamics of the single grinding body

A model for single ball impacts has been developed by Abdellaoui and Gaffet [14], determining the speed and the frequency of impacts of one single ball against the vial surface. The speed of the ball (V_b) at the collision is calculated with the equation according to [14]:

$$V_b = \sqrt{(R_d W_d)^2 + R_{eff}^2 W_v^2 \left(1 + 2\frac{W_v}{W_d}\right)} \quad (1)$$

where R_d and W_d are the radius and the rotation speed of the disc wheel, respectively. R_{eff} is the effective vial radius and W_v the rotation speed of the vial.

The impact energy (E) is then calculated as

$$E = \frac{1}{2} m_b V_b^2 \quad (2)$$

where m_b is the mass of one ball. The power of single ball impacts (P) is written as

$$P = fE \quad (3)$$

where f is denoted as the frequency of single ball impacts and is calculated by using computer facilities (for details see [14]).

2.2. Energy input in the case of multiple grinding bodies

When more than one ball is used, the number of milling balls N must be taken into account. In this case, an additional filling parameter $0 < \delta < 1$ has been introduced. This parameter characterises the dissipation of the specific impact energies due to the ball–ball interactions. The limiting value of $\delta = 1$ is when only one ball is involved and $\delta = 0$ when the vial is full and no movement of balls is possible. By normalising with the mass of powder (m_p) the energy input for the unit powder amount can be estimated. A normalised total input energy (E_n) for milling is obtained by multiplying with the milling time t

$$E_n = \frac{PNt}{m_p}\delta \quad (4)$$

In this work a first approximation of the filling parameter is done using the following linear relationship:

$$\delta = 1 - n_v \quad (5)$$

where $n_v = N/N_{tot}$ is the normalised number of balls. N_{tot} is the maximum number of balls that can be contained as a cubic arrangement in the milling vial [11], which is given by the following equation

$$N_{tot} = \frac{\pi D_v^2 H_v}{4 d_b^3} \quad (6)$$

where D_v and H_v are the diameter and the height of the vessel, respectively and d_b is the ball diameter.

Obviously the total input energy E_n in Eq. (4) is not quantitatively characterising the true energy transfer from the balls to the powder. When considering that the other variables (temperature, probability of powder particle to be in the collision, the angle of the hit, variation of the powder properties during milling, the effect of rolling, etc.) are constant or insignificant in the studied range, then Eq. (4) can be used.

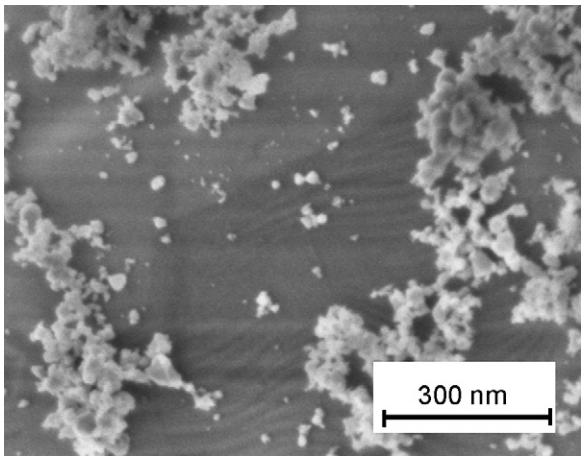

Fig. 1. SEM picture of inductively coupled plasma synthesized silicon carbide nanopowders.

3. Experimental procedure

Aluminium powder with a purity ≥99.5% and fraction of less than 65 μm (AS 011, Ecka Granules) have been used as the matrix. SiC nanoparticles (as shown in Fig. 1) have been produced in an ICP reactor as described in [15]. The mean grain size S_{BET} is ~30 nm. Powders produced by ICP are well suited for nanocomposites as the technology can be well up scaled to an industrial scale production [16].

The constituent powders were milled in a laboratory planetary ball mill (PM400, Retsch GmbH) under argon, using stearic acid (S.A.) or heptane as Process Control Agent (PCA). The loading and unloading of the powders were performed in a glove box, under argon. Because some powder was lost during the collecting manipulations (e.g. during separating the powder from the vessel or during cleaning the balls), a process yield was not assessed. The residual stearic acid after milling was estimated by weighing the amount of S.A. after rinsing with heptane and drying. The main fixed parameters for the planetary milling are given in Table 1. Whereas the parameters that have been varied in this study can be seen in Table 2.

For calculations, the weight of all the milling balls was measured before milling and divided by the number of balls. The average weight of one new ball was 4.1 and 32.6 g for 10 and 20 mm balls, respectively. The amount of wear from the milling media was calculated from the weight difference of the balls before and after milling. This was done by electronic scale with a resolution of 0.01 g. As the wear of the balls as well as the vessel has been measured to be negligible (lower than 0.2 wt.% of the milled powder for the balls and not detectable for the vessel), the wear has minor influence on the hardness of the samples.

The milled powders were consolidated by hot pressing into bulk samples of 30 mm in diameter and thickness of ~3.5 mm. The powders were sampled into the pressing die made of hot work tool steel. The powder beads in the dies were resistance heated up to a temperature of 350 °C at atmospheric pressure under air. After

Table 1
Constant milling parameters.

Parameter	Property	Value
Disc wheel	Effective radius	300 mm
Vial-to-disc speed ratio		−2:1
Grinding vials	Volume	250 ml
	Material	Stainless steel
	Radius	37.5 mm
Milling balls	Material	100Cr6 hardened steel

Table 2
Values used for milling parameters.

Variable	Unit	Range
Disc speed of rotation, W	rpm	180; 260; 360
Milling time, t	h	2. . .20
Ball diameter, d	mm	10; 20
Ball to powder ratio (BPR)		3.2:1. . .80:1
Normalised nb. of balls, N/N_{tot}		0.08. . .0.65
Process control agent (PCA)	wt.%	1.5 S.A; 20 heptane

Table 3
Milling parameters for distributed experimental space.

Input parameters					Compacts				Input Energy
Speed (rpm)	Time (h)	Ball Ø (mm)	BPR[a]	PCA[b]	Powder mass (g)	Milling time/pause (min)	Density (%)	Hardness ($HV_{0.5}$)	E_n ($Wh\,g^{-1}$)
260	2	10	10:1	Heptane	20	10/10	96.6	99.0	1.16
260	20	20	10:1	Heptane	40	20/10	96.6	83.7	10.15
360	2	20	5:1	Heptane	40	10/10	97.7	88.1	1.51
360	20	10	5:1	Heptane	20	20/10	98.4	85.4	18.59
260	2	10	5:1	S.A.	40	20/10	99.1	47.4	0.41
260	20	20	5:1	S.A.	20	10/10	98.2	138.4	7.30
360	2	20	10:1	S.A.	20	20/10	98.0	108.2	1.82
360	20	10	10:1	S.A.	40	10/10	98.8	87.9	1.46

[a] Ball to powder ratio.
[b] Process control agent.

a holding time of 1 h required for temperature homogenization of the powder, the dies were rapidly transported to the uniaxial press for subsequent compaction. The transfer duration was kept constant for all the samples, being in the order of 4–5 s. Compaction was done by applying a pressure of 570 MPa for 10 s of holding time.

The Vickers microhardness of the bulk composites was measured at 0.5 N using at least five measurements per sample. The density of the compacted materials was measured by the Archimedes method, according to the standard ISO 3369:1975.

4. Results and discussion

In order to study the effects of varying milling parameters, this work was divided into three steps. Initially the main influencing parameters were evaluated. Secondly the speed and time of milling were investigated. For these steps the low level of filling was maintained because of the predicted higher significance of single ball dynamics. Finally the influence of the number of balls and the amount of powder in the vessel were investigated. All results were combined to optimise the input energy model incorporating the studied input parameters and the experimentally determined filling parameters.

4.1. Verification of the main processing variables for milling

The initial experimental values and parameters studied in this work were based on an orthogonal experimental design (Taguchi Design). The objective was to establish experimental factors that were distributed with sufficient width to cover the experimental space. The experimental factors and values are presented in Table 3. Also the calculated value of the normalised input energy (E_n) from Eq. (4) and the main outputs–hardness and density of the pressed compacts are given in Table 3.

The results show distinctive differences depending on the used process control agents (PCA) (Table 3, Fig. 2). When using heptane as PCA, there was no sticking of aluminium on the vessel and the balls. Welding of the powder particles was found to be the dominating mechanism during the milling. As a result, large pellets with diameter of 2–7 mm were produced. The pellet size was found to be dependent on ball size and on the time of milling. The Archimedes density of the pellets was in the range from 92 to 95% of the theoretical density.

The hardness of the compacted materials when milling with heptane was not greatly influenced by the input energy (see Fig. 2). For a better mixing, it seems that milling balls with smaller diameter and moderate speeds are needed.

When using S.A as PCA, a remarkable difference (compared to using heptane) of hardness response was found. It is known that S.A. has a tendency to react during high-energy milling, introducing carbon to the powder mixture [17]. Therefore, it is assumed that reaction kinetics in addition to mixing is contributing to the hardening of the densified materials.

The increase in hardness with increasing input energy E_n with S.A. as the PCA was the subject for further studies. The milling- and pause-interval was fixed at 10/10 min, as it had a minimal contribution to the hardness.

4.2. Influence of milling speed and time

For determining the effect of milling time, speed and ball diameter, experiments with a normalised number of balls of $n_v = 0.08$ for 10 mm balls and $n_v = 0.16$ for 20 mm balls were selected. The milling period was varied between 2 and 20 h. Ball to Powder Ratio (BPR) was maintained at 10:1 and an amount of 10 or 20 g of powder was used for 10 or 20 mm balls, respectively. The different weights of balls and powder for milling with 10 or 20 mm balls were selected in order to keep the calculated normalised input energy values in the similar range. This must be kept in mind when comparing the hardness results of milling with 10 and 20 mm balls in Fig. 3A and B.

The hardness generally increases with the time and the speed of milling (Fig. 3). The milling speed has a higher influence when the milling is performed with smaller balls. For higher milling speeds, the smaller ball size seems to be more beneficial, yielding higher hardness values.

Fig. 4 shows the hardness data represented in Fig. 3A and B versus the predicted input energy E_n (Eq. (4)). The results show a clear increase in hardness up to a plateau at ~130 $HV_{0.5}$, excluding for 10 mm balls at 180 rpm (designated in Fig. 4). It is assumed that due to the low energy ($E = 0.0317$ J) for single ball impacts at this

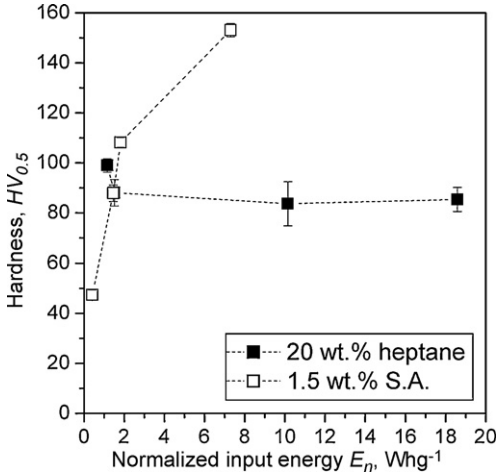

Fig. 2. Hardness of the bulk composites as a function of the total normalised input energy.

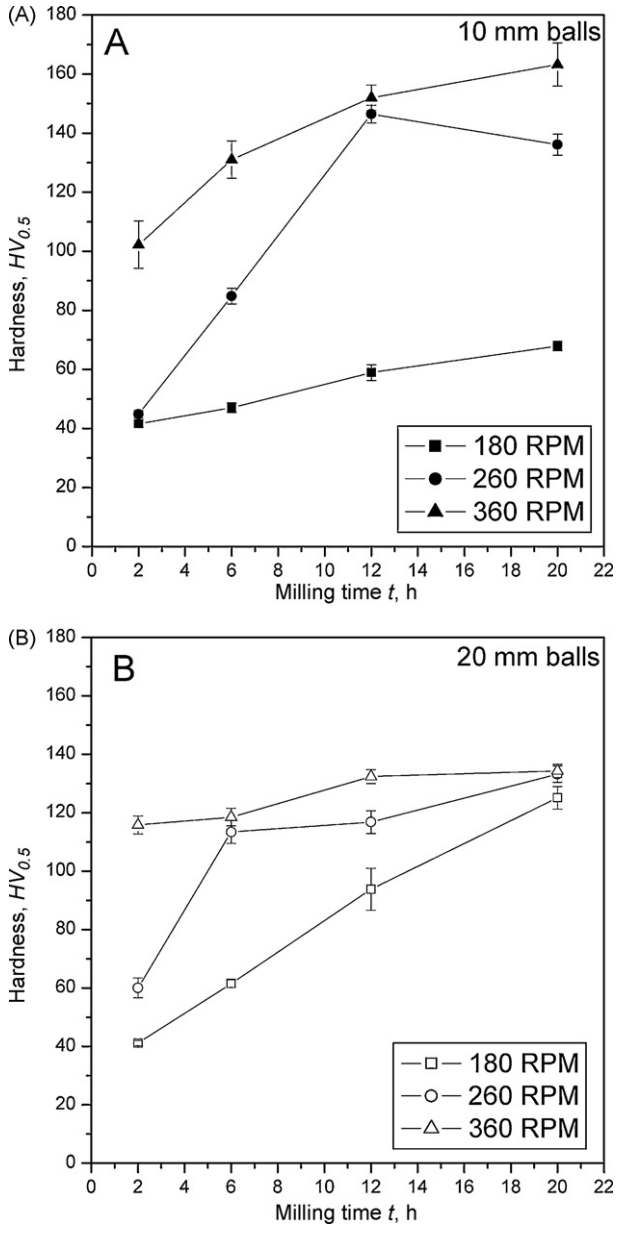

Fig. 3. Hardness of compressed samples versus milling time. (A) 10 mm balls; (B) 20 mm balls.

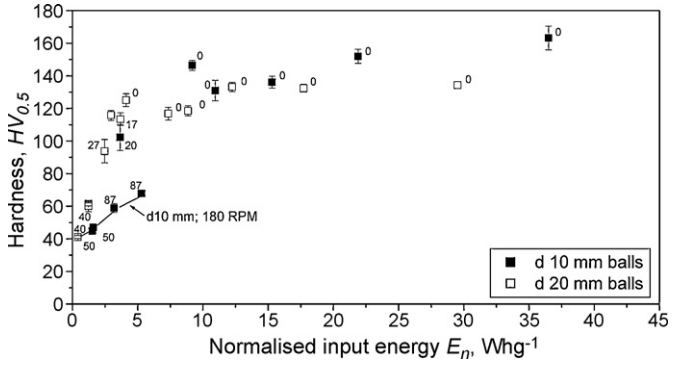

Fig. 4. Hardness versus total normalised input energy of multiple ball impacts. Designations next to the data points are indicating the amount of S.A. weighed after solution debinding (wt.%).

Table 4
Variables for establishing experimentally the filling parameters for milling with d10 and d20 mm balls.

Pos.	n_v	Powder mass (g)	BPR
1	0.13	10	16:1
2	0.13	50	3.2:1
3	0.26	20	16:1
4	0.26	40	8:1
5	0.38	30	16:1
6	0.51	20	32:1
7	0.51	40	16:1
8	0.64	10	80:1
9	0.64	50	16:1

low speed, the ability to deform and fracture the powder particle is hindered and the milling mechanisms are changed from the high-energy mode to a low energy mode. This is supported by the fact that even after 20 h of milling a high amount of S.A. was removed by debinding (between 40 and 87 wt.%).

At low input energy, the hardening of compacted samples seems to be governed by reaction kinetics of S.A. The amount extracted from the powder is gradually decreasing up to the point of about 4–5 Wh g^{-1} of input energy E_n (Fig. 4). At higher energies no S.A. could be extracted. Also, due to the loss of lubricating effect of S.A., some sticking on the vessel and the balls was observed for samples milled with input energies (E_n) higher than ~5 Wh g^{-1}.

After the reaction of all the PCA, further gradual hardening of the composites was observed, up to 163 $HV_{0.5}$ for the highest energy input. Here also it clearly appears that 10 mm balls lead to higher hardnesses than 20 mm balls.

For estimating the hardening effect from reacted stearic acid, additional tests were performed. The pure aluminium powders without the reinforcement were milled with 10 mm balls at the highest input energies (360 rpm; 12 and 20 h of milling, E_n of 21.9 and 36.5 Wh g^{-1}, respectively) so that all the stearic acid would be reacted. The hardness for these materials was measured to be 100.4 ± 3.2 and 108.9 ± 1.4 $HV_{0.5}$, for 12 and 20 h of milling, respectively. From the hardness difference between the reinforced and pure aluminium under the same milling conditions, it can be assumed that the homogenous distribution of 1 vol.% of SiC nanoparticles would contribute around 50.60 $HV_{0.5}$. The full reaction of 1.5 vol.% S.A. would be for about 55.65 $HV_{0.5}$, as the hardness of the unmilled and hot pressed aluminium was found to be 47.2 (±3.2) $HV_{0.5}$. These two enhancement effects for the hardness are accumulated in the final composite.

4.3. Constitution of the vial filling parameter by experimental data

The normalised input energy using linear relationship for the filling parameter δ with a linear relationship (Eq. (5)) showed a good agreement with the hardness response when milling was performed with a low number of balls (Figs. 2 and 4). An attempt was made to evaluate experimentally the true vial filling parameter also for higher number of balls in the vial. Therefore, a design of experiment involving normalised number of balls (n_v) from 0.13 up to 0.65 and BPR of 3.2:1– 80:1 for 10 and 20 mm balls was designed (Table 4). The speed of rotational was kept at 360 rpm and the milling time at 4 h.

4.3.1. Optimised input energy model

The optimised energy input model for total normalised input energy (E_{opt}) is given by

$$E_{opt} = \frac{PNt}{m_p}\delta_{opt} \quad (7)$$

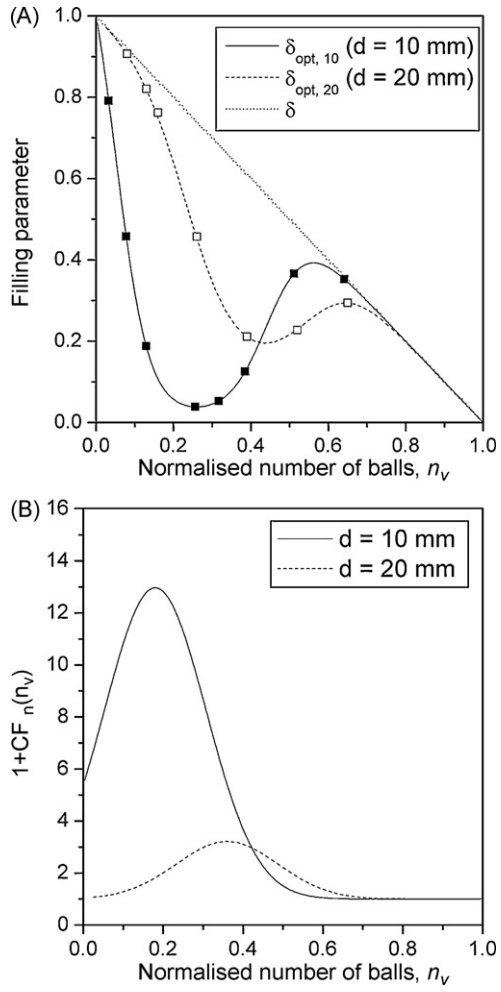

Fig. 5. Optimised filling parameters (A) and fitted Gaussian functions (B) for 10 and 20 mm steel balls. The closed and open marks in (A) are showing the fitting points used for 10 and 20 mm balls, respectively.

with the filling parameter δ_{opt} (Eq. (7)) fitted to the hardness data. The optimised filling parameters for 10 and 20 mm balls were determined experimentally. This was done by fitting the hardness data from the experimental plans where the number of balls was varied (Tables 3 and 4) with the values of the constant filling parameters (shown in Fig. 4). The linear filling parameter and the normal density were found to influence the optimised filling parameter (δ_{opt}) as

$$\delta_{opt} = (1 - n_v)^{[1+C_i F_n(n_v)]} \tag{8}$$

where $F_n(n_v)$ is the density of the normal distribution:

$$F_n(n_v) = \frac{1}{\sigma\sqrt{2\pi}} \exp\left(-\frac{(n_v - \mu_i)^2}{2\sigma^2}\right) \tag{9}$$

The subscript i is nominating the used ball diameter (10 or 20). The constant C_i characterising the weight of the function $F_n(n_v)$ was fitted with $C_{10} = 2.7$ and $C_{20} = 0.6$. The mean and the deviation of the Gaussian function were found to approach $\mu_{10} = 0.18$, $\mu_{20} = 0.36$ and $\sigma = 0.09$, respectively. The fitted Gaussian function and the resultant optimised filling parameters are shown in Fig. 5A and B, respectively. The resulting energy input–hardness relationship, after implementation of the fitting procedures, are shown in Fig. 6. For the normalised number of balls n_v, the parameter characterising the vessel being completely full (N_{tot}), was calculated to be 309 and 39 for the 10 and 20 mm balls, respectively.

A remarkable decrease of filling parameter is spotted for 10 mm balls whereas it is less pronounced for 20 mm balls up to the vial filling limit of 0.25 and 0.42, respectively (Fig. 5A). After the local minima, the filling parameters increase again, up to the second maximum at $n_v = 0.58$ and 0.63 for 10 and 20 mm balls, respectively (Fig. 5A). The highest normalised number of balls studied in this work was at $n_v = 0.64$. At higher number of balls, further decrease in filling parameter is expected for the expected evolution of close packed formation of balls.

Previous works on planetary milling have shown that the character of ball motion and impacts depend on the number of balls in the vial [18–20]. At low balls filling in the vessel, mainly the shear forces are found to contribute to the energy dissipation. When the number of balls is increased, the prevailing normal impacts are recorded. This transformation has been explained by the formation of ordered structures of balls when milling with higher filling levels [18].

The curves for filling parameters are in good agreement with the significance of normal impacts (as predicted in [18,19]) for the further increase of filling parameters at 0.23–0.64 and 0.39–0.64 for 10 and 20 mm balls, respectively. Nevertheless, the curves obtained in this work have remarkable differences to the ones found previously for mechanical alloying [11,21] or mechanochemical reactions [19]. For these applications, the non-hindering region for up to ~20% of normalised number of balls was found, where ball–ball interactions do not affect the filling parameter [19,21]. The highest amount of consumed energy of ball impacts (measured by the temperature output) has been estimated to be at n_v of ~0.3 in the case of [16]. In the present study this is the area that should be avoided as yielding the lowest hardness values.

A recent study of Jiang et al. [20] was investigating the area of low filling of the vial. Their results on the energy transfer from the balls are in agreement with the results in this work for a low number of balls. Indeed increasing the number of balls, a decrease in consumed energy was found. The local minimum of consumed energy was recorded at the filling level of n_v ~0.16 for 10 mm balls in a 500 ml vessel.

The minimum for the filling parameter δ_{opt} was found to be 0.04 for 10 mm balls and 0.20 for 20 mm balls. The lower significance of filling parameter for larger diameter balls (in Fig. 5A) can be explained by the consideration of the ball energies by rolling. Especially for the larger ball sizes, the rolling has found to contribute to the consumed energy [18].

According to the remarks above there are indications on the importance of both the normal and shear forces during milling. For a low number of balls the shear forces are dominating and, for higher loading, the normal forces are prevailing during milling. But it must be mentioned that the occurrence of local minima for filling parameters is still unclear.

4.3.2. Hardness and powder morphology response to optimised input energy

After implementation of the fitting procedures, the hardness versus optimised input energy was obtained (Fig. 6). The curve seems to present at least three regions. At low energy no evolution of the hardness is observed. Thus for E_{opt} between ~0.7 and 3 Wh g^{-1} the hardness increases before reaching a plateau again at higher energies. However, considering the powder morphology, the milling may be divided into four regions according to the input energy. The examples of the powder structure evolution versus the input energy of milling for 10 and 20 mm balls has been highlighted in Fig. 6, and shown in Fig. 7A and B. The milling with 10 mm balls at 260 rpm is highlighted with rounded grey areas in Fig. 6 and the according morphologies as shown in Fig. 7A. For the 20 mm balls, the speed of 180 rpm was chosen, highlighted with rectangular patterned areas in Fig. 6. The according morphologies are shown in

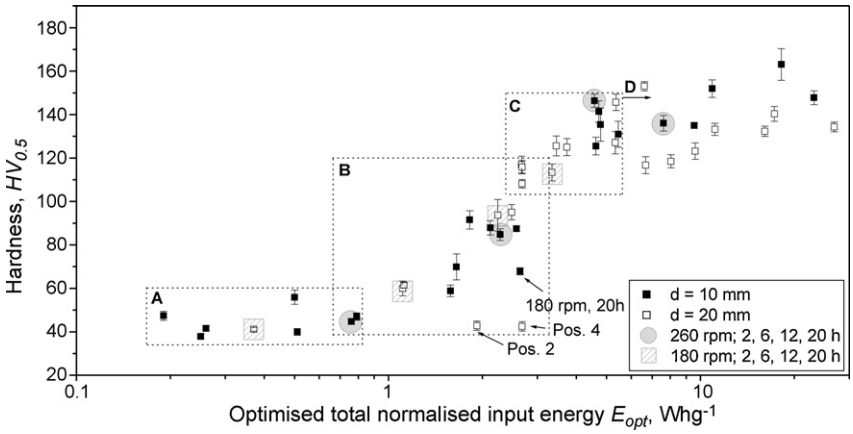

Fig. 6. Hardness of the pressed samples as a function of optimised total normalised input energy. Powder structure development is shown in four regions: Region A, flattening of the powder particles; Region B, plastic deformation and cold welding of the particles. Transformation phase from flake like- to rounded structure; Region C, stabilisation phase for the formation of the equiaxed particles; Region D, equilibrium state for fracturing-welding of the particulates. The highlighted data points are showing the milling with 10 mm balls at 260 rpm (round grey) and 20 mm balls at 180 rpm (rectangular patterned) for different times of milling.

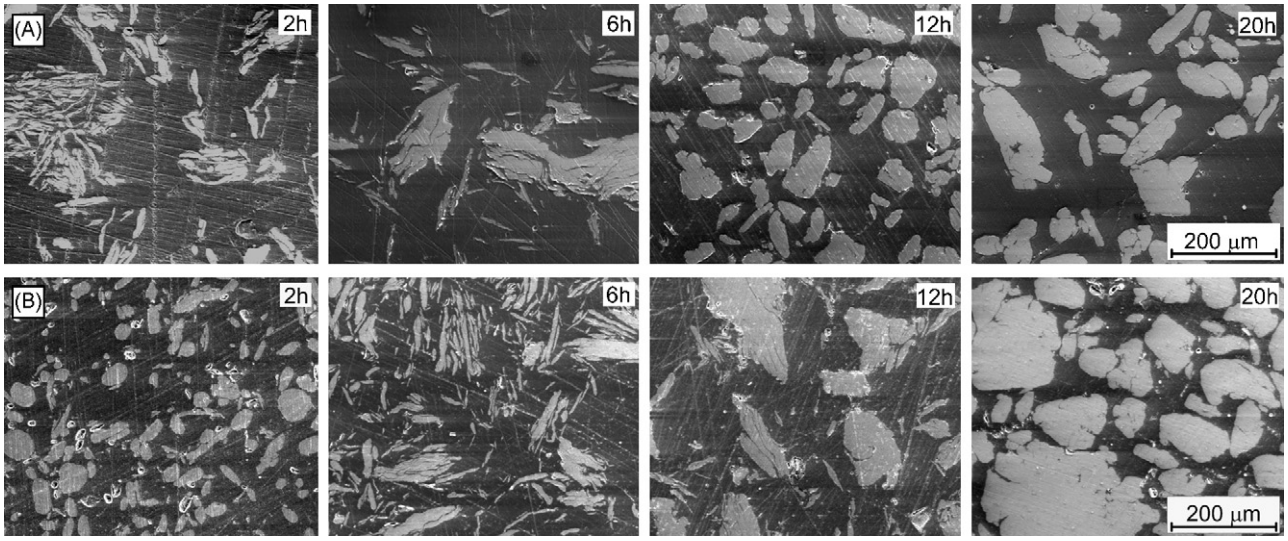

Fig. 7. Structure of the powders milled with A: d = 10 mm balls at 260 rpm; and B: d = 20 mm balls at 180 rpm. Designations at the upper right corner of the SEM images are describing the hours of milling.

Fig. 7B. The results are in accordance with previous findings considering the structure evolution of metal matrix composite powders as a function of milling time [9].

Region A (E_{opt} < ~0.9 Wh g^{-1}): Flattening of the powder due to the plastic deformation of the particles. No hardening of the compacts is found. The representative powder morphologies are depicted in Fig. 7B – 2 h and Fig. 7A – 2 h.
Region B (0.7 < E_{opt} < 2.5 Wh g^{-1}): Transformation from the flake like to spherical powder due to plastic deformation and cold welding of the particles. The hardness is increased due to the combined effect of reaction of S.A. and mixing with SiC nanoparticles. The representative structures through the region are shown in Fig. 7A – 2–6 h and Fig. 7B – 6–12 h.
Region C (2.5 < E_{opt} < 5.5 Wh g^{-1}): Formation of the spherical powder morphology due to the plastic deformation and fracture of the particles. All the S.A. is reacted and the lubricating effect of the S.A. is lost. Further increase in the hardness is observed. Microstructure images in Fig. 7A – 12 h and Fig. 7B – 20 h are illustrating the powder morphologies in this region.
Region D (E_{opt} > ~5.5 Wh g^{-1}): The particles going through further plastic deformation is diminished. The equilibrium state between fracture and welding of particles is achieved. No considerable hardness enhancement is accompanied. The hardness properties in this region depend mainly on the mixing state achieved in the previous regions (assuming that all the carbon addition from S.A. has been homogeneously distributed). It seems however that milling with smaller diameter balls contributes to a better mixing during the early stages of milling. The maximum hardness values at highest input energies with 10 mm balls were found to outperform the values for the ones obtained with 20 mm balls.

For two cases in region B, a deviation from the main curve was observed (indicated with arrows in Fig. 6). The first deviation was found in the case of milling at the speed of 180 rpm with 10 mm balls (as indicated with "180 rpm, 20 h" in Fig. 6). It is assumed that there is a certain threshold for single ball impact energies from which lower values do not yield sufficient energy allowing the reaction of S.A.

A second deviation from the model was found for the lower ball to powder ratios and lower number of balls for a milling with 20 mm balls (positions 2 and 4 in Table 4, designated as Pos 2 and 4 in Fig. 6). Probably here the impact energy will be dissipated in the powder bed, inhibiting the particle deformation. Clearly one factor

for filling parameter would also be the amount of powder in the mill, which has not been studied in this work.

Basing on the above data, some suggestions can be proposed for increasing the hardness of Al-nanoSiC materials while minimising the milling time. When the highest powder output in minimum time is desired, larger balls, highest speed and normalised number of balls of 0.6–0.7, just above the local minimum are recommended. Considering that somewhat higher hardness results were obtained with 10 mm balls, smaller balls and normalised number of balls n_v at 0.5–0.6 are recommended in the case of the milling configuration used in this study.

5. Conclusions

The hardness development of the Al–1 vol.%nanoSiC system has been studied during a planetary milling. It was found that the selection of the process control agent has a significant effect on the powder morphology and on the hardness of the hot compacted samples. When stearic acid is used, micron sized composite powders are obtained. Heptane instead enhances the welding of the powders during milling, yielding in millimetre sized pellets. The hardness for the materials milled with stearic acid is influenced by the mixing with the SiC nanoparticles and from the reaction of the stearic acid during milling. The hardness increases with the input energy. When milling with heptane no remarkable influence of the input energy on the hardness was observed in the studied range.

The influence of different processing parameters was studied for milling with the addition of 1.5 wt.% of stearic acid as the process control agent. A model for energy input was introduced and further optimised. Therefore, a vial filling parameter was determined experimentally. All parameters studied in this work—speed, time of milling, mass of balls and powders, and ball diameter were found to contribute to the hardness development.

A pronounced decrease in energy transfer from the balls to the powder was found with an increasing the number of balls, when the milling is performed at low vial filling levels. A local minimum of vial filling parameter was found when milling with either 10 or 20 mm balls. This was recorded at vial filling of 0.25 and 0.42 for 10 and 20 mm balls, respectively. Further addition of milling balls again improved the amount of transferred energy, yielding in higher milling efficiency. By optimised milling parameters, introducing the highest input energies with smaller diameter balls, a fourfold increase in the composite hardness at 163 $HV_{0.5}$ was achieved. As a comparison, hot compressed pure aluminium showed the value of 47.2 ($\pm$3.2) $HV_{0.5}$.

Acknowledgement

This work was supported by the Gerbert Rüf Stiftung (grant no. GRS 019/07).

References

[1] S.C. Tjong, Adv. Eng. Mater. 9 (8) (2007) 639–652.
[2] S. Kamrani, A. Simchi, R. Riedel, S.M. Seyed Reihani, Powder Metall. 50 (2007) 276–282.
[3] Z.R. Hesabi, H.R. Hafizpour, A. Simchi, Mater. Sci. Eng. A 454–455 (2007) 89–98.
[4] C. Suryanarayana, Prog. Mater. Sci. 46 (1–2) (2001) 1–184.
[5] B.Q.H.F. Tang, M. Hagiwara, J.M. Schoenung, Adv. Eng. Mater. 9 (4) (2007) 286–291.
[6] F. Tang, M. Hagiwara, J.M. Schoenung, Mater. Sci. Eng. A 407 (1–2) (2005) 306–314.
[7] J.A. Rodriguez, J.M. Gallardo, E.J. Herrera, J. Mater. Sci. 32 (13) (1997) 3535–3539.
[8] H. Abdoli, E. Salahi, H. Farnoush, K. Pourazrang, J. Alloys Compd. 461 (1–2) (2008) 166–172.
[9] K. Gan, M. Gu, J. Mater. Process. Technol. 199 (1–3) (2008) 173–177.
[10] B.S. Murty, M. Mohan Rao, S. Ranganathan, Acta Metall. Mater. 43 (6) (1995) 2443–2450.
[11] N. Burgio, A. Iasonna, M. Magini, S. Martelli, F. Padella, Il Nuovo Cimento D 13 (4) (1991) 459–476.
[12] O. Boytsov, E. Gaffet, F. Bernard, A. Ustinov, J. Alloys Compd. 432 (2007) 103–110.
[13] T.H. Courtney, Mater. Trans. JIM 36 (2) (1995) 110–122.
[14] M. Abdellaoui, E. Gaffet, Acta Metall. Mater. 43 (3) (1995) 1087–1098.
[15] Y. Leconte, M. Leparoux, X. Portier, N. Herlin-Boime, Plasma Chem. Plasma Process. 28 (2) (2008) 233–248.
[16] D. Vollath, J. Nanopart. Res. 10 (2008) 39–57.
[17] S. Kleiner, F. Bertocco, F.A. Khalid, O. Beffort, Mater. Chem. Phys. 89 (2–3) (2005) 362–366.
[18] E.V. Shelekhov, V.V. Tcherdyntsev, L.Y. Pustov, S.D. Kaloshkin, I.A. Tomilin, International Symposium on Metastable Mechanically Alloyed and Nanocrystalline Materials (ISMANAM-99), Trans Tech Publications Ltd., Dresden, Germany, 1999, pp. 603–608.
[19] M.P. Dallimore, P.G. McCormick, International Symposium on Metastable Mechanically Alloyed and Nanocrystalline Materials (ISMANAM-96), Transtec Publications Ltd., Rome, Italy, 1996, pp. 5–13.
[20] X. Jiang, M.A. Trunov, M. Schoenitz, R.N. Dave, E.L. Dreizin, J. Alloys Compd. 478 (1–2) (2009) 246–251.
[21] A. Iasonna, M. Magini, Acta Mater. 44 (3) (1996) 1109–1117.